PHYSICAL REVIEW B VOLUME 6, NUMBER 6 15 SEPTEMBER 1972

Radiation Damage in $KMgF_3 : KMnF_3$ †

W. E. Vehse*
Solid State Division, Oak Ridge National Laboratory, Oak Ridge, Tennessee 37830

and

W. A. Sibley
Department of Physics, Oklahoma State University, Stillwater, Oklahoma 74074
(Received 7 January 1972)

Optical absorption, bleaching, and annealing studies of mixed crystals of $KMgF_3 : KMnF_3$ irradiated at 80 °K with 2.0-MeV electrons are reported. It was found that the presence of Mn suppresses the F-center production mechanism in $KMgF_3$. At concentrations of Mn greater than 1.4 at.%, the absorption spectrum is dominated by a set of five bands originating from a single type of defect. A possible model for this defect involving an F center trapped between adjacent Mn ions is discussed. Limited studies of the $KMgF_3 : KZnF_3$ system were made for purposes of comparison.

I. INTRODUCTION

Over the past years considerable effort has been expended in research on radiation-induced defects in alkali halides.[1,2] Through these studies the various radiation products such as F, $F_2(M)$, and $F_3(R)$ centers have been identified and used to unravel the mechanism for the production of radiation damage in these materials.[3] More recently similar work has been done on alkaline-earth oxides[4,5] and fluorides,[6,7] and again information has been obtained which not only elucidates the radiation-damage mechanism in these substances, but in some cases leads to means of making the materials more radiation resistant. It is our feeling that the experimental techniques and careful characterization methods of this type of research should be extended into those materials which have potential usefulness as devices. The purpose of this paper is to present data that will show why it is difficult to produce radiation damage in materials such as $KMgF_3$: Mn and $KMnF_3$.

Recently, the F-, F_2-, F_3-, and $X_2^-(V_K)$-center absorption bands have been identified in $KMgF_3$[8,9] and the radiation-damage mechanism has been studied. This material behaves under irradiation in a manner similar to alkali halides, and the dominant radiation-damage mechanism is that of radiolysis. However, it has been observed by several investigators that the structural isomorphs of $KMgF_3$ and MgF_2 which contain Mn are either not readily damaged or else the damage does not show up as F centers.[10,11] Two possible reasons for this behavior of the Mn salts are (i) that the radiolysis production mechanism is suppressed due to energy being lost to Mn^{2+} optical transitions, much as Pooley has shown a suppression of the mechanism in KI when energy is lost to luminescence,[12] and/or (ii) that an F center adjacent to a Mn^{2+} ion has a strongly perturbed optical-absorption band which is not easily observed. Our study of $KMg_x Mn_{1-x} F_3$ crystals was begun in order to decide which of the above possibilities is correct. In addition, limited studies of the system $KMg_x Zn_{1-x} F_3$ were carried out for purposes of comparison to aid in identifying the role played by the Mn ion.

II. EXPERIMENTAL

The crystals used in these experiments were grown by the Stockbarger technique.[10] $KMgF_3$ and $KMnF_3$ form solid solutions in all proportions and reasonable sized crystals of optical quality were obtained.[13] The system $KMgF_3 : Zn$ was found more difficult to grow. Most of the samples used were in the form of 0.75-mm-thick single crystals cleaved along a (100) plane. (Polycrystalline slices were used for the 0.57 at.% Zn and 29.6 and 45.6 at.% Mn samples.[14]) The impurity analyses were essentially the same as shown in Ref. 9.

All irradiations were performed at 80 °K in a Sulfrian cryostat using a Van de Graaff electron accelerator operated at 2.0 MeV. Dose rates for the growth curves were 1.85×10^{13} MeV/cm^3 sec. Calibration was done by comparison with previous work under similar conditions on $KMgF_3$.[9,10]

Bleaching experiments were performed using a mercury arc with appropriate interference filters. Polarization was obtained using the same source with unsupported Polaroid HNPB ultraviolet sheets. Optical measurements were made with Cary 14R and 15 spectrophotometers and with a Jarrell-Ash monochromator. In all cases the natural linewidths were greater than the instru-

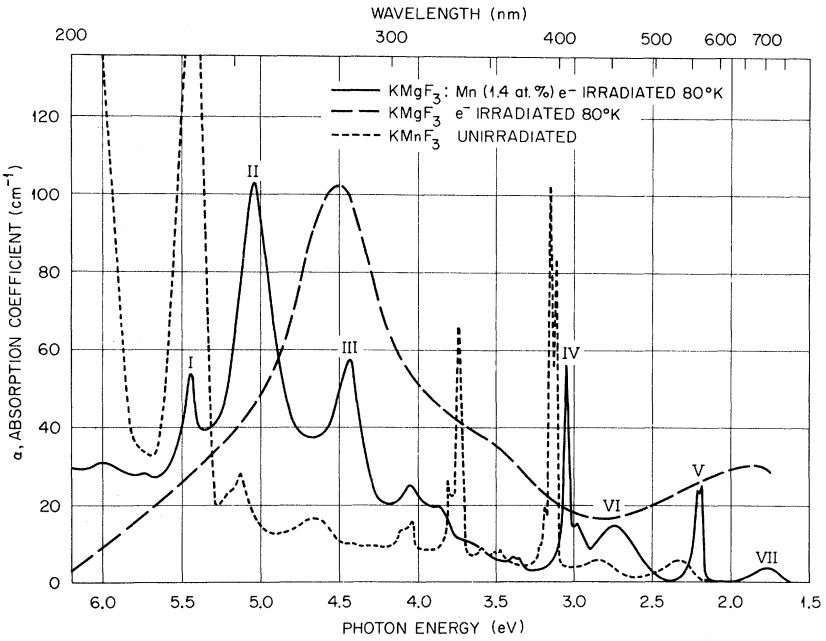

FIG. 1. Plot of the absorption coefficient vs photon energy for a $KMgF_3$: Mn (1.4 at.%) crystal electron irradiated at 2.0 MeV and 80 °K (solid line). Spectra of $KMgF_3$ irradiated under similar conditions (dashed line) and unirradiated $KMnF_3$ (dotted line) are shown for comparison.

ment resolution.

III. RESULTS

A. Spectra

The irradiation-induced absorption spectrum of $KMgF_3$: $KMnF_3$ crystals is complex, even for the case of low-temperature irradiations. This survey is limited to those features of the spectra which appear to be common to the entire range of compositions and which continue to grow after prolonged irradiation.

The absorption spectrum for an irradiated crystal containing 1.4 at.% Mn is illustrated as the solid curve in Fig. 1. Shown for comparison are the absorption spectra for an *irradiated* pure $KMgF_3$ crystal and for *unirradiated* pure $KMnF_3$. The five bands labeled I–V are the only ones studied in detail. Bands VI and VII are associated with the presence of Mn in the lattice, but they grow in rapidly and then decrease with radiation dose. Moreover, these bands are not seen in pure $KMnF_3$. The structure between bands III and IV is too weak to be studied conveniently in most of the mixed crystals.

Irradiation of crystals of $KMgF_3$ at 80 °K produces the spectrum shown by the long-dashed curve in Fig. 1. The broad band at 273 nm has been identified as the *F* band.[9] Irradiated crystals doped with 0.4 at.% Mn exhibit this same *F* band with the addition of the five bands I–V. As seen in Fig. 1, when the concentration of Mn has reached 1.4 at.% the five-band spectrum is dominant. There is probably some *F*-band absorption under bands II and III, as can be inferred from the optical-bleaching experiments to be discussed later.

As the Mn content is increased, all of the bands shift in position, as shown in Fig. 2. There is also a broadening of the bands with increasing Mn concentration. For example, band *V* increases in half-width from 435 cm^{-1} at 1.4 at.% Mn to 800 cm^{-1} for pure $KMnF_3$.

Crystals containing 1.4 at.% Mn show considerable structure when measured at 7 °K in the vicinity of bands IV and V. This is evident in the main panels of Fig. 3. Reduction of the Mn level to 0.4 at.% enhances this structure and allows the observation of a series of regularly spaced (2.5×10^{-3} eV) lines near the peak of band V, as shown in the inset to Fig. 3. A similar series of equally spaced (16×10^{-3} eV) lines is observed on the low-energy side of band IV in both the 0.4 and 1.4 at.% Mn crystals.

For purposes of comparison, crystals of $KMgF_3$ doped with Zn were irradiated under conditions identical to those for the Mn-doped crystals. As shown in Fig. 4, two bands in addition to the *F* band were observed, one with a peak at 333 nm and a second near the absorption edge at 230 nm. The complex visible portion of the spectrum observed in Mn-doped crystals was not seen in the Zn-doped crystals.

B. Growth Curves

Growth curves for the *F* band in $KMgF_3$ (doped and pure), irradiated at 80 °K, are shown in Fig.

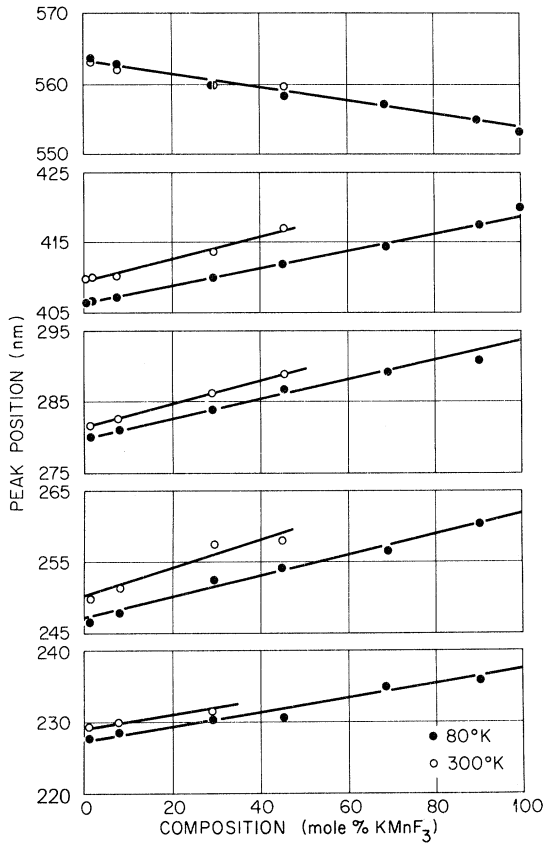

FIG. 2. Plot of peak position vs percentage $KMgF_3$ for bands I–V in $KMgF_3:KMnF_3$ crystals.

5. It is of interest to note that, whereas the effect of the Zn impurity is to enhance the early stage colorability, as in the case of the impurity-doped alkali halides (e.g., Pb-doped KCl[15]) the presence of Mn as an impurity leads to a suppression of the coloration rate. The growth of the F band in a 1.4 at.% Mn crystal is not directly measurable, since, as previously discussed, at this composition the spectrum is dominated by the Mn-associated bands.

In order to determine if the suppression with impurity doping was due to a short circuiting of the production mechanism, a closely related experiment was performed. Divacancies (F_2 centers) were introduced by a room-temperature irradiation; then the crystal was cooled to 80 °K and irradiated. At this temperature the F_2 centers formed by the 300 °K irradiation are no longer in radiation equilibrium with F centers and consequently are destroyed by capturing interstitials produced during irradiation. The more interstitials that are produced, the greater is the destruction rate for the F_2 centers. The results of this experiment are shown in the inset. Values of the F_2 absorption coefficient, normalized to the initial value, are plotted as a function of radiation dose. Although the results for the 1.4 at.% Mn crystal are uncertain because of the growth and then destruction of a Mn-associated band (band VI, Fig. 1) during the course of the irradiation, it is apparent that the F_2 annihilation rate for this crystal is significantly lower than that of pure $KMgF_3$. The bars indicate the extreme values obtained by applying (a) no correction for the presence of band VI (upper value) and (b) the maximum possible, and clearly excessive, correction (lower value).

Growth rates for the Mn-associated band at

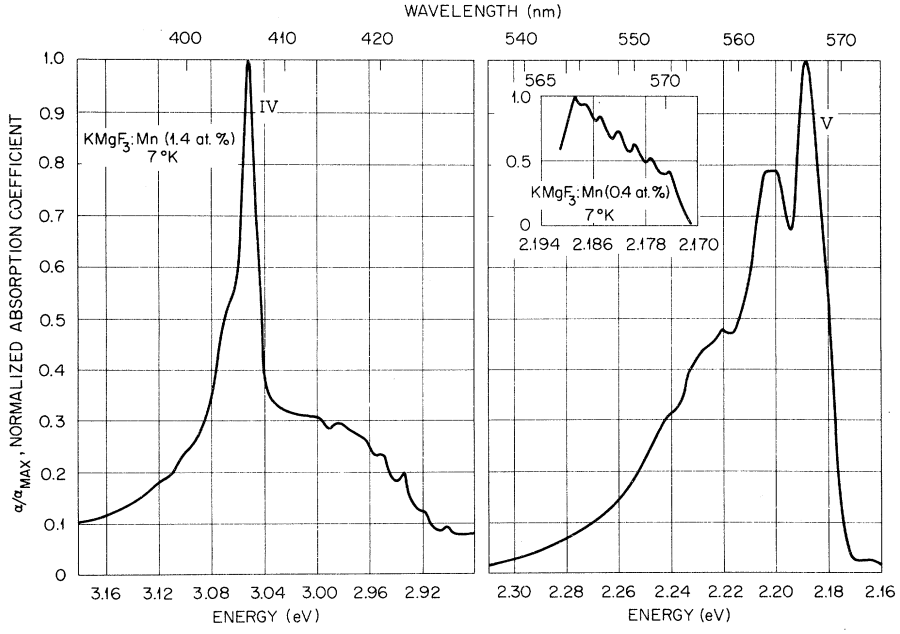

FIG. 3. Plot of normalized absorption coefficient vs photon energy for bands IV and V in a $KMgF_3$: Mn (1.4 at.%) crystal irradiated at 80 °K. The inset shows the structure which appears near the peak of band V for lower Mn concentrations.

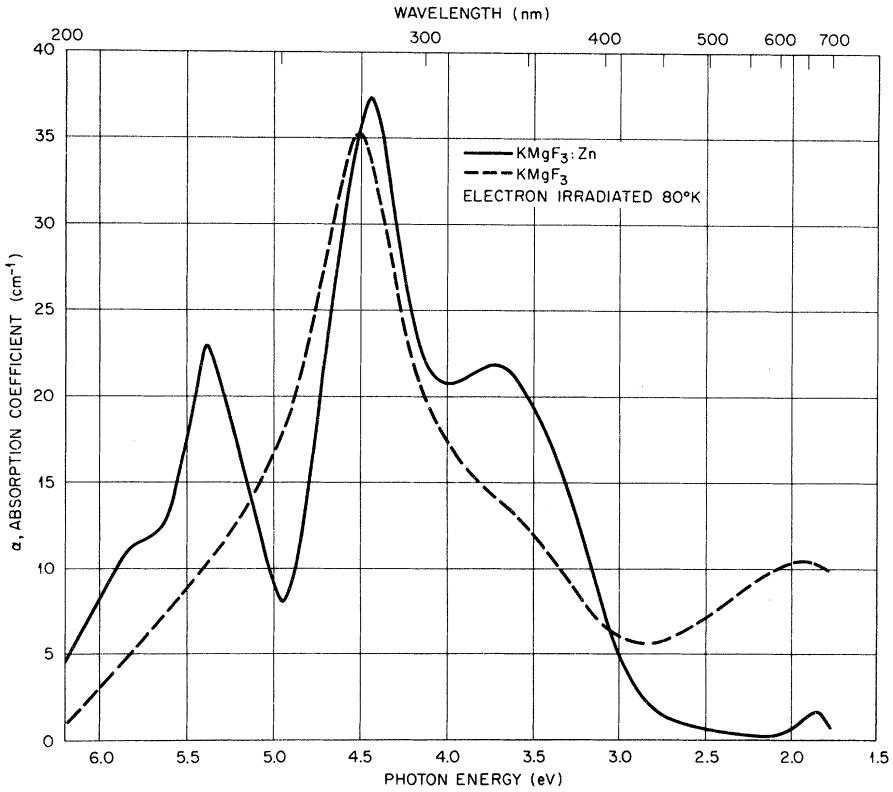

FIG. 4. Plot of the absorption coefficient vs photon energy for a $KMgF_3$: Zn (0.57 at.%) crystal electron irradiated at 2.0 MeV and 80 °K (solid line). The spectrum of $KMgF_3$ irradiated under similar conditions (dashed line) is shown for comparison.

~565 nm (band V) are shown in Fig. 6. By way of comparison, the growth rate for the *F* band in pure $KMgF_3$ is given by the nearly vertical dashed line. Since the line shapes of the bands for all of the compositions are similar, a plot of the product of the half-width and peak absorption co-

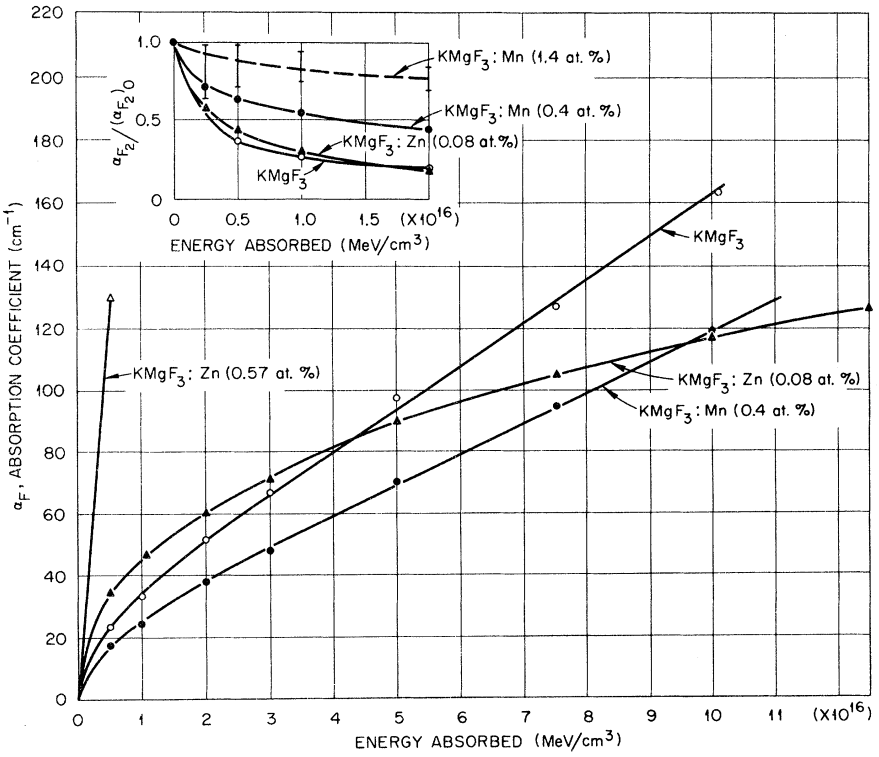

FIG. 5. Plot of the *F*-center absorption coefficient vs radiation dose for several doped and one pure crystal electron irradiated at 2.0 MeV and 80 °K. The inset shows the normalized approach to equilibrium for a nonequilibrium distribution of F_2 centers irradiated under similar conditions.

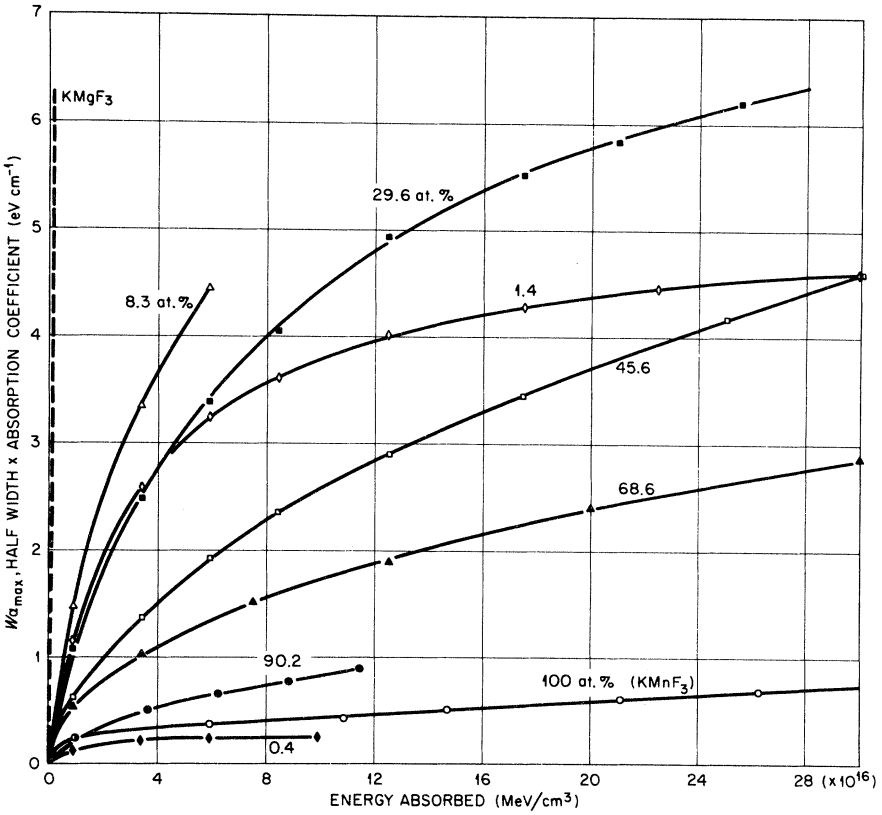

FIG. 6. Plot of the relative total absorption vs radiation dose for band V in $KMgF_3:KMnF_3$ crystals electron irradiated at 2.0 MeV and 80 °K. The dashed line is the corresponding curve for the F band in pure $KMgF_3$.

efficient, rather than area under each curve, is adequate to give relative values. Of the five prominent irradiation bands, the 565-nm band (band V) is the easiest to analyze, since it is relatively free from underlying bands. Within experimental error, all other bands show similar growth rates.

For the lowest doping level, the growth curve of the 565-nm band quickly saturates. Saturation is also observed in the 1.4 at.% Mn crystal and even in the 29.6 at.% Mn sample. The growth rate first increases with the Mn content, reaching a maximum between 1.4 and 29.6 at.%, then decreases to the rate observed in pure $KMnF_3$. The growth curve for $KMnF_3$ was continued to twice the dose indicated by the last point with no observable departure from linearity.

C. Bleaching

Bleaching $KMgF_3$ in the F-band region at room temperature converts the F centers to F_2 and higher-aggregate centers.[9] This effect was also observed for 0.08 at.% Zn- and 0.4 at.% Mn-doped crystals. For higher concentrations of Zn and Mn, however, conversion of F centers to F-aggregate centers was suppressed by conversion to impurity centers. Figure 7 shows the room-temperature spectra of a 1.4 at.% Mn-doped

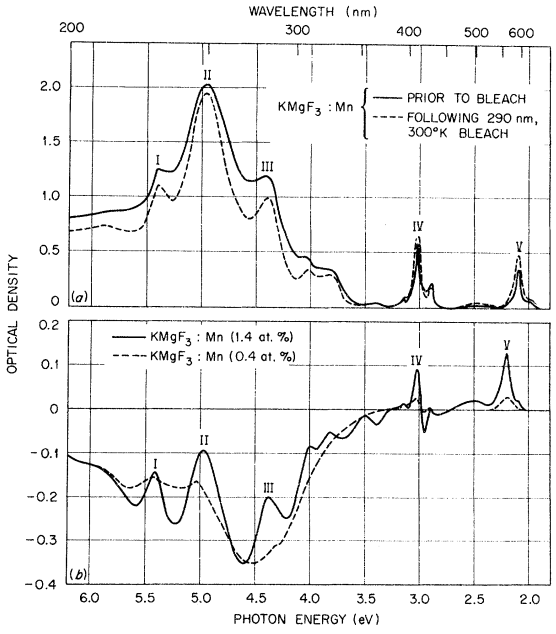

FIG. 7. (a) Effect of a room-temperature, 290-nm unpolarized bleach on a $KMgF_3:Mn$ (1.4 at.%) crystal previously electron irradiated at 2.0 MeV and 80 °K. (b) Difference curve obtained from (a) by subtraction of the absorption curve prior to bleaching from the curve following bleaching (solid line). Difference curve for a $KMgF_3:Mn$ (0.4 at.%) crystal (dotted line).

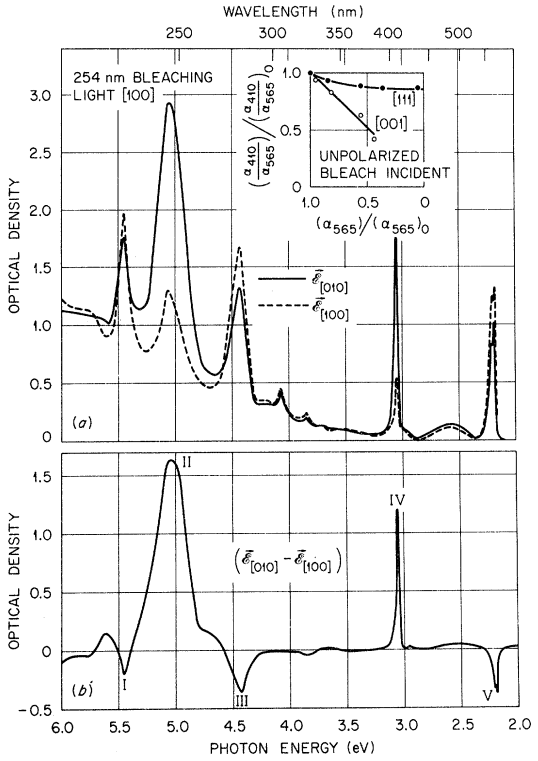

FIG. 8. (a) Effect of a room-temperature polarized bleach on a previously irradiated $KMgF_3$: Mn (1.4 at.%) crystal. Bleaching light propagating along [001], polarized along [100]. Measuring light polarized along [010] (solid line) and along [100] (dotted line). (b) Difference curve obtained from (a) by subtraction of [100] measured spectrum from [010] spectrum. Inset shows effect of crystal orientation on the relative destruction of bands IV and V in an unpolarized bleaching experiment.

crystal before and after a 290-nm bleach. The difference curve shown in the lower portion of the figure is obtained by subtraction. Negative values therefore are indicative of an annihilation of centers; positive values (or positive peaks on a generally negative curve) indicate new centers have been produced. The difference curve shows a broad decrease in the F-band region and, superimposed on this decrease, a growth of the five Mn-associated bands. The corresponding difference curve for the 0.4 at.% Mn crystal is shown by the dashed curve in Fig. 7(b). For this crystal, the decrease in the F band is much more apparent, while the increase in the Mn-associated bands is evident in the uv region only as slight "bumps" on the difference curve.

D. Polarization

The most prominent bands in the irradiation spectrum for the Mn-doped samples are polarizable. The centers responsible for these lines can be aligned by bleaching at room temperature with linearly polarized 254-nm light, propagating along [001] with the electric vector $\vec{\mathcal{E}}$ along [100] or [010]. There is no tendency toward alignment, when the electric vector of the incident light is along [110]. This definitely established the symmetry of the centers as ⟨100⟩.[16] The polarization is observed easily in the 1.4 at.% Mn samples as seen in Fig. 8. These curves were obtained by measuring the absorption of polarized light at 80 °K following a 2-h 300 °K bleach. The dichroism $\vec{\sigma}_{[010]} - \vec{\sigma}_{[100]}$ is illustrated in the lower portion of the figure. Note that bands I, III, and V are polarized parallel to the electric vector of the bleaching light, while II and IV are polarized perpendicular to this direction. Polarization could also be observed in the 0.4, 68.6 at.% Mn, and pure $KMnF_3$ crystals, although in $KMnF_3$, bands I–III are so weak relative to the intrinsic Mn spectrum (Fig. 1) and to a broad easily produced radiation band,[10] that only the polarization of IV and V was observed. Polarization at room temperature is accomplished by a selective destruction of centers rather than a reorientation. Bleaching, whether polarized or not, followed by a short reirradiation does not restore the number of centers to its prebleached value as would be the case if the defects were not actually destroyed.

E. Annealing

Isochronal annealing studies were performed only on the 1.4 at.% Mn crystals with the results for bands IV and V depicted in Fig. 9. Annealing times were 10 min at the temperature shown. The samples were quenched to 23 °C, where all measurements were made, by removing them from the furnace and onto a copper block. The separation of the curves above 150 °C is real and indicates the presence of a small underlying broader band in the 410-nm region. The bands I–III anneal concurrently within experimental error. As the Mn content is increased, the thermal stability of the bands decreases, so that for the 68.6-, 90.2-at.% Mn, and pure-$KMnF_3$ crystals, the irradiation bands are nearly destroyed when the sample is warmed from 80 °K to room temperature.

IV. DISCUSSION

Two general conclusions can be drawn from the observations presented in this paper: (i) The presence of manganese impurities in $KMgF_3$ suppresses the radiolysis production of interstitial-vacancy pairs, and (ii) at least five of the irradiation-induced bands observed in $KMgF_3$: Mn crystals (bands labeled I–V in the text) are due to Mn impurity–F-center complexes.

The radiolysis mechanism for radiation damage

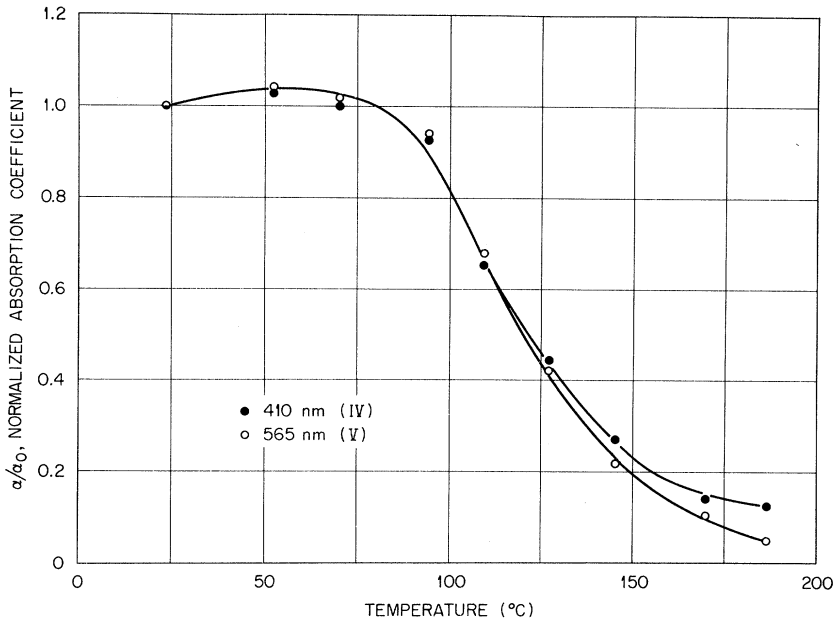

FIG. 9. Isochronal annealing curve for bands IV and V in a $KMgF_3$: Mn (1.4 at.%) crystal electron irradiated at 2.0 MeV and 80 °K.

in halide crystals is now reasonably well understood, due to the work of Pooley, Hersh, and Luschik and their co-workers.[2,3] Frenkel pair production is triggered by the formation of $X_2^-(V_K)$ centers and the recombination of these hole centers with electrons. If some of the recombination energy is lost due to luminescence or recombination in the presence of certain impurities,[12] then the remaining energy is insufficient to displace a halogen from its lattice site and create a Frenkel pair. On the other hand, if enough recombination energy can be focused along preferred directions at the time of the electron-hole recombination, the halogen can be ejected into an interstitial site, and at temperatures approaching the liquid-nitrogen boiling point, will diffuse through the lattice. Thus, there are two aspects to the radiation-damage process in these materials: The first aspect is the radiolysis production mechanism, and the second is the motion of the interstitial and its subsequent interaction with impurities, other interstitials, and vacancies. As an example pertinent to this study, if a greater than equilibrium concentration of F_2 centers can be formed in a crystal, then irradiation of this crystal will return it to its equilibrium concentration of F and F_2 centers very rapidly, since the interstitials produced by radiolysis will annihilate with the vacancies, destroying F_2 centers and thus forming F centers.

The data presented in Fig. 5 suggest that Mn impurities act to suppress the radiolysis production mechanism at low temperatures. The main panel shows that the F-center growth curve for the 0.4 at.% Mn-doped sample is lower than that of pure $KMgF_3$. The growth curves for crystals with larger Mn concentrations cannot be obtained directly, because the F band is masked by bands I–III. However, the growth rate for the F band in a 1.4 at.% Mn-doped crystal is estimated by a subtraction process to be no more than 50% of the rate for the pure crystals. Since the unfilled $3d$ shells of the Mn^{2+} ions have many optical transitions both in the ultraviolet and visible regions of the spectrum, and since the X_2^- center has a high probability of being formed in the vicinity of a Mn ion for the concentrations studied, it is not unlikely that much of the energy which would normally be available to the halogen for displacement is used up in exciting the Mn transitions. In order to check this possibility, a $KMgF_3$ crystal was doped with Zn impurities and irradiated in the same manner as the other specimens. The main panel of Fig. 5 reveals that Zn impurities do not act in the same manner as the Mn. In fact the F-center growth curve is enhanced. The enhancement is probably due to impurity trapping of interstitials which would result in a decrease in the vacancy-interstitial annihilation. Since Zn has a filled $3d$ shell, we would not expect energy from the X_2^- center electron recombination to be used up in exciting optical transitions in this impurity. Riley[10] has observed a suppression of the F-center production rate in Mn-doped crystals in room-temperature irradiations. This room-temperature suppression could arise from the same mechanism as proposed for the low-temperature irradiations.

The inset in Fig. 5 is a plot of the decrease of

the excess F_2-center concentration, introduced by irradiation at 300 °K and cooling to 80 °K, as a function of radiation dose and impurity. It should be noted that the Mn-doped samples show a slower decrease than the pure $KMgF_3$ specimens. This fact is consistent with the model that fewer interstitials are produced in the Mn-doped material, although the results could also be explained by increased impurity trapping.

Previous experiments on alkali halides have shown that at temperatures below the mobility temperature of the X_2^- center, impurity doping leads to an enhancement of the coloration. This has been explained as being due to interstitial trapping by impurities; above this temperature the X_2^- centers are mobile and can move to impurities, where recombination with an electron occurs and a quenching or suppression of the radiolysis mechanism takes place. In this experiment a suppression of the coloration was found at radiation temperatures below that of the mobility of the X_2^- center (~ 110 °K). This is not surprising, since the impurity concentration is so high and the X_2^- wave functions are so diffuse that even for immobile X_2^- centers there will be an interaction with Mn ions. However, it should be noted that Still and Pooley[17] found that the coloration mechanism in KCl could be suppressed by heavy doping of impurities due to a disruption of the focusing sequence, which displaced the interstitial far enough from its vacancy to prevent correlated recombination. The perovskite structure is not as amenable to focusing as the rock-salt structure and so replacement sequences are not expected to play as important a role in $KMgF_3$ as in KCl. Furthermore, the replacement sequence should be disrupted by Zn impurities, as much as by Mn; and yet the production mechanism seems unaffected by Zn doping. Thus, it appears that the suppression of the radiolysis mechanism in $KMgF_3$:Mn is due to an interaction between the X_2^- centers and the Mn impurities, which results in an excitation of the $3d$ transitions of the Mn and drains off sufficient energy that the radiolysis mechanism is inefficient. At this stage of the investigation it is not known whether the mechanism is completely suppressed and the damage in the pure $KMnF_3$ is due to elastic collisions between electrons and lattice ions, or if it is just reduced in its efficiency.

The second major point for discussion concerns the origin of the bands labeled I–V in Fig. 1. The experimental evidence supports the following conclusions: (i) The bands arise mainly from a single type of center; (ii) the symmetry of the center is ⟨100⟩; and (iii) the center involves more than one Mn ion, probably a Mn ion pair. The data suggest that the center involved is a Mn ion-defect complex. A model of an F center trapped between a pair of Mn ions (Mn^{2+}-$\mathcal{F}$-Mn^{2+}) is proposed as a reasonable one, which can explain the experimental observations satisfactorily.

Conclusion (i) is supported by the following evidence. Within experimental error the *ratios* of the growth rates for the various bands are independent of Mn concentration and radiation dose; the annealing rates, except for the presence of a small underlying band in the 410-nm region, are identical (Fig. 9); and the bleaching rates are the same after correcting for the difference in the bleaching rates for σ and π transitions of a ⟨100⟩-type center as discussed in the Appendix. Polarized bleaching experiments definitely establish the symmetry of this center as ⟨100⟩, as discussed above.

Comparison of the spectra for the Zn-doped material (Fig. 4) with the Mn-doped crystals (Fig. 1) indicates that the Mn ion or ions are directly involved in this center. The center probably involves a pair of Mn ions, rather than a single ion, as indicated by the following experimental observations: (i) The bands (especially II, IV, and V) are observed even in pure $KMnF_3$; (ii) polarized bleaching experiments, as discussed below, indicate the centers do not reorient as would be likely for a center involving a single Mn ion, but impossible for a pair; and (iii) a saturation of the growth curves for these bands is seen for both the 0.4 and 1.4 at.% Mn-doped $KMgF_3$. From this last observation one must conclude that the number of possible sites for such centers is small. Thus, it is more likely that the defect involves Mn-impurity pairs than only isolated Mn impurities. The intensity of the absorption bands is in agreement with this concept. The $3d$ transitions in Mn are both spin and symmetry forbidden. Ferguson, Guggenheim, Tanabe[18] show that in Mn-doped $KZnF_3$, the pair transitions of the Mn ions are three orders of magnitude more intense than the single-ion spectra, because an interaction of the form $J\vec{S}_a \cdot \vec{S}_b$ between pairs of ions makes the transitions spin-allowed. Since it is likely that bands I–V have their origin in the $3d$ shells of the Mn ions, the transitions associated with a Mn pair should predominate. The structure associated with bands IV and V could be due in part to the weaker single-ion spectra, since it is observed only in the 1.4 and 0.4 at.% doped samples and is stronger relative to the main line in the lower-doped material.

A simple reasonable model for the center giving rise to the observed Mn bands is that of an F center trapped between two Mn^{2+} ions. The observed bands would then be transitions within the Mn $3d$ shell, highly perturbed by the removal of the fluorine ion and consequent lattice distortions.

The data shown in Figs. 6 and 7 lend support to such a model. The slow growth of the bands shown in Fig. 6 is indicative of the suggestion that the center involves a defect rather than a different charge state of the Mn ion. Growth curves for a process involving a simple ionization of the Mn ion should tend to saturate more readily. These curves in Fig. 6 also show that the production mechanism for the center is suppressed with increasing Mn content as is the case for the F center. The growth rates for the Mn bands are determined by the number of available sites (which increases with increasing Mn) and the production mechanism. Between 0.4 and 8.3 at.% Mn, the availability of Mn sites is dominant, while the subsequent decrease to 100 at.% Mn shown in Fig. 6 may be attributed to the suppression of the mechanism with increasing Mn. The results presented in Fig. 7 are consistent with this model in that they show that F centers may be converted to the Mn ion-defect complex by optical bleaching.

In an attempt to see if the assumption of the model of an F center trapped between two Mn ions is a reasonable one for the explanation of bands I–V, the following experimental analysis was made. Samples of $KMgF_3:Mn$ were irradiated to form F centers. The specimens were then bleached with 254-nm light polarized along [100], and it was found that anisotropic absorption in bands I–V could be produced. The bleaching also indicated that the centers were formed preferentially with [010] as the σ direction. When the polarization of the bleaching light was changed to [010], then these centers were preferentially bleached and no realignment of centers was observed, i.e., a total decrease in centers was seen and not a shift from one orientation to another. It is clear that polarization of the bleaching light will affect the alignment of the centers only after they have been created; thus, it appears that if an F center becomes trapped between two manganese ions, it remains trapped unless it is optically excited along the Mn^{2+}-$\mathcal{F}$-Mn^{2+} axis. This is not unreasonable since when the F-center electron is in the excited state, it will have a high probability of being found outside the Mn ions, and as a result there will be a relaxation of Mn impurities away from the vacancy, drawing the eight near-neighbor fluorines toward the negative-ion vacancy. This enhances the probability of a fluorine jumping into the excited F center and a destruction of the trap. This interpretation, although only one of several possibilities, seems to be the most likely and certainly is capable of explaining the data presented in this paper.

With the assumption that the above model is correct, one would expect to have both σ- and π-polarized optical transitions. The analysis given in the Appendix indicates that optical bleaching experiments using polarized and unpolarized light can uniquely distinguish between π and σ transitions. Our experiments indicate that bands II and IV are σ polarized while I, III, and V must be π transitions. As shown in the Appendix, the ratio α_σ/α_π of the absorption coefficients for the σ and π transitions of a $\langle 100 \rangle$ center bleached along [001] may be made to decrease to zero by prolonged bleaching, if the σ transitions are more effective than the π transitions in destroying the centers. If the π transitions are more effective, the ratio α_σ/α_π will double with prolonged bleaching. In the case of the 1.4 at.% Mn-doped samples in a bleaching experiment with 225-nm unpolarized light, the ratio of α_{410} (band IV) to α_{565} (band V) was found to decrease to 0.41 ± 0.05 times its initial value (Fig. 8 inset), and in a similar experiment with unfiltered mercury light, this ratio decreased by a factor of 0.31 ± 0.05. The fact that the change was more than a factor of 2 leads to the conclusions that (i) bleaching is more effective for σ transitions than for π transitions and (ii) band IV, which decreases the most, is a σ transition. It follows then that band II is also a σ transition and bands I, III, and V are π transitions. An unpolarized bleach along [111] (Fig. 8 inset) shows that the ratio $\alpha_{410}/\alpha_{565}$ remains essentially constant, indicating that the change in ratio of $\alpha_{410}/\alpha_{565}$ observed in the [001] bleach is not due to the presence of two centers. The slight decrease observed may be attributed to imperfect alignment of the crystal.

Qualitatively this assignment of the polarizations of bands I–V fits the predicted polarizations one would obtain when the site symmetry of the Mn^{2+} ion is changed from O_h to C_{4v}, as would be the case for the proposed model.[19] Band V must arise from two different π transitions, and it is seen that this band does have a complicated structure at all doping levels. A simple model involving different charge states of the Mn ion, as, for example, Mn^{1+}, in a field of C_{4v} should give rise either to a series of many closely spaced polarized lines or, if the lines are unresolved, to broad unpolarized or weakly polarized bands.

In summary we can state that Mn impurities in $KMgF_3$ suppress the coloration mechanism, and when present in large concentrations can even reduce the colorability at 80 °K. Furthermore, in crystals with high levels of Mn it is possible to form what appears to be an F center trapped between two Mn impurity ions. This trap releases when the F center is excited along the

Mn^{2+}-$\mathcal{F}$-Mn^{2+} direction, because of the outward relaxation of the Mn ions and the near-neighbor fluorines.

ACKNOWLEDGMENTS

We would like to thank C. B. Finch for the preparation of some of the Zn-doped crystals. One of us (W. E. V.) would like to express his appreciation to the members of the Solid State Division of Oak Ridge National Laboratory for providing the opportunity to pursue this research while on sabbatical leave from West Virginia University.

APPENDIX

In this Appendix a bleaching experiment is described by which it is possible to differentiate between σ and π transitions of a polarizable center. Specifically, centers with $\langle 100 \rangle$ symmetry will be discussed.

Consider a crystal containing defect centers which may be bleached, with not necessarily equal effectiveness, by electric dipole transitions both along and perpendicular to the axis of symmetry. If the bleaching light propagates along [001] and is polarized along [100], then the equations describing the bleaching of [100], [010], and [001] centers will be

$$n_x(t) = n_x(0)\, e^{-a_\sigma t} , \tag{A1a}$$

$$n_y(t) = n_y(0)\, e^{-a_\pi t} , \tag{A2a}$$

$$n_z(t) = n_z(0)\, e^{-a_\pi t} , \tag{A3a}$$

where $n(t)$ is the density of centers following a bleach of time t, and where the subscripts x, y, and z refer to [100], [010], and [001] symmetries, respectively. a_σ and a_π are coefficients describing the bleaching effectiveness of the σ and π transitions, respectively. For light propagating along [001], but polarized along [010], one would have the similar set of equations:

$$n_x(t) = n_x(0)\, e^{-a_\pi t} , \tag{A1b}$$

$$n_y(t) = n_y(0)\, e^{-a_\sigma t} , \tag{A2b}$$

$$n_z(t) = n_z(0)\, e^{-a_\pi t} . \tag{A3b}$$

For [001] unpolarized light the rates would simply be additive so that

$$n_x(t) = n_x(0)\, e^{-(a_\sigma + a_\pi)t} , \tag{A1c}$$

$$n_y(t) = n_y(0)\, e^{-(a_\sigma + a_\pi)t} , \tag{A2c}$$

$$n_z(t) = n_z(0)\, e^{-2a_\pi t} . \tag{A3c}$$

Suppose that following an unpolarized bleach for a time t, the absorption coefficients α_σ and α_π are measured for the σ and π transitions. Since $\alpha_\sigma \sim f_\sigma n_\sigma(t)$ and $\alpha_\pi \sim f_\pi n_\pi(t)$, where f_σ and f_π are the appropriate oscillator strengths and $n_\sigma(t)$ and $n_\pi(t)$ are the densities of centers which can participate in σ and π transitions, one has for unpolarized measuring light propagating along [001]

$$\alpha_\sigma \sim f_\sigma [n_x(t) + n_y(t)] \sim f_\sigma \tfrac{2}{3} N e^{-(a_\sigma + a_\pi)t} , \tag{A4}$$

$$\alpha_\pi \sim f_\pi [n_x(t) + n_y(t) + 2n_z(t)] \sim f_\pi \tfrac{2}{3} N (e^{-(a_\sigma + a_\pi)t} + e^{-2a_\pi t}) . \tag{A5}$$

In deriving Eqs. (A4) and (A5) the assumption has been made that the initial densities $n_x(0)$, $n_y(0)$, and $n_z(0)$ are each equal to $\frac{1}{3}N$, when N is the total defect density. The factor of 2 in the term $2n_z(t)$ in Eq. (A5) arises because of the fact that for unpolarized light [001] centers will have π components along both orthogonal orientations of the electric vector.

Consider the ratio

$$\frac{\alpha_\sigma(t)}{\alpha_\pi(t)} \Big/ \frac{\alpha_\sigma(0)}{\alpha_\pi(0)} = 2\, \frac{1}{1 + e^{(a_\sigma - a_\pi)t}} \tag{A6}$$

as $t \to \infty$ for

$$a_\sigma - a_\pi > 0 , \tag{A6a}$$

$$a_\sigma - a_\pi = 0 , \tag{A6b}$$

$$a_\sigma - a_\pi < 0 . \tag{A6c}$$

For (A6a),

$$\frac{\alpha_\sigma(t)}{\alpha_\pi(t)} \Big/ \frac{\alpha_\sigma(0)}{\alpha_\pi(0)} \to 0 , \tag{A7}$$

for (A6b)

$$\frac{\alpha_\sigma(t)}{\alpha_\pi(t)} \Big/ \frac{\alpha_\sigma(0)}{\alpha_\pi(0)} = 1 , \tag{A8}$$

for (A6c)

$$\frac{\alpha_\sigma(t)}{\alpha_\pi(t)} \Big/ \frac{\alpha_\sigma(0)}{\alpha_\pi(0)} \to 2 , \tag{A9a}$$

or

$$\frac{\alpha_\pi(t)}{\alpha_\sigma(t)} \Big/ \frac{\alpha_\pi(0)}{\alpha_\sigma(0)} \to \frac{1}{2} . \tag{A9b}$$

The limits expressed in (A7), (A8), and (A9b) allow for the possibility of uniquely determining the polarizations of transitions arising from the same center. Let $\alpha_1(t)$ and $\alpha_2(t)$ represent the absorption coefficients of orthogonally polarized transitions as a function of bleaching time t. Further, let $\alpha_1(t)$ be assigned to the transition which decreases most rapidly. Then if $[\alpha_1(t)/\alpha_2(t)]/[\alpha_1(0)/\alpha_2(0)]$ becomes less than $\frac{1}{2}$, Eq. (A6a) is applicable; $(a_\sigma - a_\pi) > 0$ and $\alpha_1(t)$ must be associated with a σ transition [Eq. (A7)]. If $[\alpha_1(t)/\alpha_2(t)]/[\alpha_1(0)/\alpha_2(0)]$ approaches $\frac{1}{2}$ after a prolonged bleach, Eq. (A6c) is applicable; $(a_\sigma - a_\pi) < 0$ and $\alpha_1(t)$ is associated with a π transition [Eq. (A9b)]. If $\alpha_1(t)/\alpha_2(t) = \text{const}$, a_σ and a_π are equal and no determination is possible.

†Research sponsored jointly by the National Science Foundation and U. S. Atomic Energy Commission under contract with Union Carbide Corp.

*Guest scientist from Physics Department, West Virginia Univ., Morgantown, W. Va. 26506.

[1]J. H. Schulman and W. D. Compton, *Color Centers in Solids* (MacMillan, New York, 1962).

[2]J. H. Crawford, Advan. Phys. 17, 93 (1968).

[3]E. Sonder and W. A. Sibley, in *Defects in Solids*, edited by J. H. Crawford and L. Slifkin (Plenum, New York, 1972).

[4]B. Henderson and J. E. Wertz, Advan. Phys. 17, 749 (1968).

[5]A. E. Hughes and B. Henderson, in Ref. 3.

[6]P. Gorlich, H. Karras, Ch. Symanowski, and P. Ukman, Phys. Status Solidi 25, 92 (1968).

[7]W. A. Sibley and O. E. Facey, Phys. Rev. 174, 1076 (1968).

[8]T. P. P. Hall and A. Leggeat, Solid State Commun. 7, 1657 (1969).

[9]C. R. Riley and W. A. Sibley, Phys. Rev. B 1, 2789 (1970).

[10]C. R. Riley, Ph. D. dissertation (University of Tennessee, 1970) (unpublished).

[11]A. E. Hughes (private communication).

[12]D. Pooley, Solid State Commun. 4, 351 (1965); Proc. Phys. Soc. (London) 87, 245 (1966); 247 (1966).

[13]W. E. Vehse, F. Sherrill, and C. R. Riley, J. Appl. Phys. 43, 1320 (1972).

[14]All percentages refer to the fraction of Mg and Mn sites occupied by Mn ions. Stated another way, the values quoted are the mole percentages of $KMnF_3$ in mixture.

[15]E. Sonder and W. A. Sibley, Phys. Rev. 140, A539 (1965).

[16]W. D. Compton and H. Rabin, in *Solid State Physics*, edited by F. Seitz and D. Turnbull, (Academic, New York, 1963), Vol. 16.

[17]P. B. Still and D. Pooley, Phys. Status Solidi 32, 147K (1969).

[18]J. Ferguson, H. J. Guggenheim, and Y. Tanabe, J. Phys. Soc. Japan 21, 692 (1965).

[19]F. A. Cotton, *Chemical Applications of Group Theory* (Wiley, New York, 1963).

PHYSICAL REVIEW B VOLUME 6, NUMBER 6 15 SEPTEMBER 1972

Coloration Induced in MgO by MeV $^{20}Ne^+$ Bombardment

Bruce D. Evans, James Comas, and Philip R. Malmberg
Naval Research Laboratory, Washington, D. C. 20390
(Received 13 March 1972)

The coloration produced near room temperature in MgO by 1.0- to 4.8-MeV $^{20}Ne^+$ bombardment has been investigated. Energetic Ne^+ ions incident upon crystalline MgO induce point defects on the anion sublattice primarily through atomic collisions. An electron(s) trapped in the anion vacancy forms an F-type center producing a characteristic, intense optical-absorption band near 5 eV. This point-defect lattice damage is restricted primarily to a thin layer of material approximately 1 to 2 μ thick located 2 to 4 μ beneath the bombarded surface. Average F-type-center volume concentrations in this thin layer range from 4×10^{18} to 5×10^{19} cm^{-3} resulting from a Ne^+ dose range of 10^{13} to 3×10^{16} ions/cm^{-2}. F-type-center production is relatively inefficient; it is estimated that 5 keV are expended per center produced, in the low-dose range, assuming centers are created only by atomic collision processes. The peak F-type-center volume concentration saturates near 10^{20} cm^{-3} resulting from a dose of 10^{16} ions/cm^2 at 3-MeV energy. This concentration level is followed by a decrease upon subsequent bombardment. A similar saturation effect is observed for a 574-nm absorption band. A quadratic dependence between the growth of the intensity of the F-type center and that of the 574-nm band suggests the latter is associated with a divacancy. Volume-concentration saturation levels for both bands are independent of many impurities commonly present in this material. Isochronal annealing results demonstrate that both bands have annealed out at 600 °C. Comparison is made with previously reported fast-neutron irradiations and the present work. Point defects on the cation sublattice, such as the V^- center, were sought for but determined not to be present in sufficient concentration to be detected by the presence of the well-known 2.3-eV optical-absorption band.

I. INTRODUCTION

Radiation damage in MgO has been studied extensively by several workers during the past decade.[1-3] Both Van de Graaff electron irradiation and fast-neutron irradiation produce an intense optical-absorption band near 250 nm. This band has been assigned to an F-like center. More careful work by Kappers, Kroes, and Hensley[4] has shown that the 250-nm band is in fact composed of two closely spaced bands, one at 250.0 nm and the other at 246.5 nm measured at 80 °K. The former is assigned to the F^+ center, one electron trapped at an oxygen vacancy,[3] the latter to the F center, two electrons trapped at an oxygen vacancy. Since these two centers are different